AD-A020 358

# TEMPERATURE COMPENSATED PIEZOELECTRIC MATERIALS

G. R. Barsch, et al

Pennsylvania State University

Prepared for:

Air Force Cambridge Research Laboratories

15 July 1975

DISTRIBUTED BY:

NTIS

National Technical Information Service
U. S. DEPARTMENT OF COMMERCE

043220

ADA020358

AFCRL-TR-75-0609

# TEMPERATURE COMPENSATED PIEZOELECTRIC MATERIALS

G. R. Barsch
K. E. Spear

MATERIALS RESEARCH LABORATORY
The Pennsylvania State University
University Park, Pennsylvania 16802

Semi-Annual Technical Report No. 1

15 July 1975

Approved for public release; distribution unlimited

Sponsored by

Defense Advanced Research Projects Agency
ARPA Order No. 2826

DDC
FEB 10 1976

Monitored by

AIR FORCE CAMBRIDGE RESEARCH LABORATORIES
AIR FORCE SYSTEMS COMMAND
UNITED STATES AIR FORCE
HANSCOM AFB, MASSACHUSETTS 01731

Reproduced by
NATIONAL TECHNICAL
INFORMATION SERVICE
U.S. Department of Commerce
Springfield, VA 22151

ARPA Order Number

2826

Program Code Number

5D10

Name of Contractor

The Pennsylvania State University

Effective Date of Contract

January 31, 1975

Contract Number

F19628-75-C-0085

Principal Investigators and Telephone Numbers

G. R. Barsch, (814) 865-1657

K. E. Spear, (814) 865-1198

AFCRL Project Scientists and Telephone Numbers

P. H. Carr, (617) 861-2527

A. F. Armington, (617) 861-2908

Contract Expiration Date

March 31, 1977

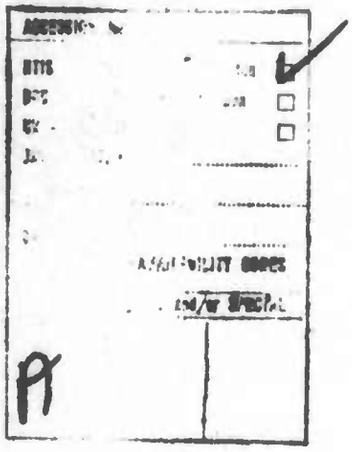

Qualified requestors may obtain additional copies from the Defense Documentation Center. All others should apply to the National Technical Information Service.

SECURITY CLASSIFICATION OF THIS PAGE (When Data Entered)

| REPORT DOCUMENTATION PAGE | | READ INSTRUCTIONS BEFORE COMPLETING FORM |
|---|---|---|
| 1. REPORT NUMBER<br>AFCRL-TR-75-0609 | 2. GOVT ACCESSION NO. | 3. RECIPIENT'S CATALOG NUMBER |
| 4. TITLE (and Subtitle)<br>TEMPERATURE COMPENSATED PIEZOELECTRIC MATERIALS | | 5. TYPE OF REPORT & PERIOD COVERED<br>Scientific - Interim<br>1 January 75-30 June 75 |
| | | 6. PERFORMING ORG. REPORT NUMBER<br>Semi Annu Tech Rpt No. 1 |
| 7. AUTHOR(s)<br>G.R. Barsch<br>K.E. Spear | | 8. CONTRACT OR GRANT NUMBER(s)<br>F19628-75-C-0085 |
| 9. PERFORMING ORGANIZATION NAME AND ADDRESS<br>The Pennsylvania State University<br>207 Old Main<br>University Park, Centre County, PA 16802 | | 10. PROGRAM ELEMENT, PROJECT, TASK AREA & WORK UNIT NUMBERS<br>2826-n/a-n/a |
| 11. CONTROLLING OFFICE NAME AND ADDRESS<br>Air Force Cambridge Research Laboratories<br>Hanscom AFB, Massachusetts 01731<br>Contract Monitor: Dr. Paul Carr/LZM | | 12. REPORT DATE<br>15 July 75<br>13. NUMBER OF PAGES<br>34 |
| 14. MONITORING AGENCY NAME & ADDRESS (if different from Controlling Office) | | 15. SECURITY CLASS. (of this report)<br>Unclassified<br>15a. DECLASSIFICATION/DOWNGRADING SCHEDULE |

16. DISTRIBUTION STATEMENT (of this Report)

Approved for public release; distribution unlimited

17. DISTRIBUTION STATEMENT (of the abstract entered in Block 20, if different from Report)

18. SUPPLEMENTARY NOTES

This research was sponsored by the Defense Advanced Research Projects Agency. ARPA Order No. 2826

19. KEY WORDS (Continue on reverse side if necessary and identify by block number)

Crystal growth; Elastic Constants; Thermoelastic Constants; Temperature Compensated Materials; Barium Germanium Titanate; Barium Silicon Titanate; Lead Potassium Niobate; Eucryptite; Berlinite.

20. ABSTRACT (Continue on reverse side if necessary and identify by block number)

In order to search for new temperature compensated materials for surface acoustic wave (SAW) devices with low ultrasonic attenuation and high electromechanical coupling, the following experimental investigations were carried out:

(1) Crystal growth experiments were performed on $Ba_2Ge_2TiO_8$, $Ba_2Si_2TiO_8$ and $Pb_2KNb_5O_{15}$. Single crystals of $Ba_2Ge_2TiO_8$ and of $Pb_2KNb_5O_{15}$ of sufficient size and quality for property measurement were obtained.

DD FORM 1 JAN 73 1473 EDITION OF 1 NOV 65 IS OBSOLETE

Unclassified

SECURITY CLASSIFICATION OF THIS PAGE (When Data Entered)

(2) For α-berlinite, $ALPO_4$, measurement of the single crystal elastic constants, their temperature dependence, and the temperature dependence of the thermal expansion coefficient was completed, and estimates of the piezoelectric constants were obtained. The results indicate that temperature compensated cuts for bulk waves should exist with orientations similar to those for the AT and BT cuts in α-quartz, and that the corresponding electromechanical coupling factors should be up to 250 percent larger than for α-quartz.

(3) For β-eucryptite, $LiAlSiO_4$, the single crystal elastic constants were measured as a function of temperature and pressure. The temperature and pressure coefficients of all elastic constants are negative. No temperature compensated cuts for bulk waves were found, and the electromechanical coupling is expected to be small. The temperature coefficient of time delay for bulk waves was small due to the negative coefficient of thermal expansion.

TEMPERATURE COMPENSTAED PIEZOELECTRIC MATERIALS

## Technical Summary

### (1) Technical Problem

In the past few years surface acoustic wave (SAW) devices have been developed and applied to perform a variety of signal processing functions, including (but not restricted to) correlation, pulse compression and matched filtering. Applications of SAW devices include communications and Radar systems, such as multichannel communications, secure anti-jam communications, miniature avionics and electromagnetic counter measures.

The performance of SAW devices is based on the generation and propagation of Raleigh-type surface waves on a substrate consisting of a piezoelectric material. The substrate material most widely used at present is α-quartz because in α-quartz temperature compensated cuts exist which result in performance characteristics independent of temperature, and which are essential for applications in which transmitter and receiver operate at different temperatures. However, the relatively low electromechanical coupling factor of α-quartz limits the operating frequency and/or bandwidth of SAW devices and constitutes a serious disadvantage.

The objective of the work under this contract is to search for new temperature compensated piezoelectric materials for use in SAW devices with properties superior to those of α-quartz, that is with larger electromechanical coupling, and with ultrasonic attenuation smaller than, or comparable to that of α-quartz.

### (2) Methodological Approach

Exploratory and systematic crystal growth experiments have been started in order to obtain single crystal specimens of a group of potentially useful materials that have been selected earlier under AFCRL Contract F 19628-73-C-108 on the basis of theoretical considerations. The single crystal specimens

are intended for the measurement of the pertinent physical properties, also to be performed under the present contract, especially of the elastic, thermoelastic, piezoelectric and dielectric properties, in order to determine suitability of these materials and their superiority to α-quartz for SAW devices.

(3) Technical Results

During the first six months of the present contract, research on the following topics was performed:

A. Crystal Growth: The crystal growth effort centered on $Ba_2Ge_2TiO_8$, $Ba_2Si_2TiO_8$, and $Pb_2KNb_5O_{15}$. Both Bridgman and Czochralski crystal growth experiments were performed, and large good quality crystals of $Ba_2Ge_2TiO_8$ were obtained from the latter pulling experiments. The quality of these crystals is hampered by a core in the boules. $Ba_2Si_2TiO_8$ was synthesized in polycrystalline form, and initial growth experiments were carried out. Attempts to grow $Pb_2KNb_5O_{15}$ continued, but cracking has remained a problem. The cracking problems in $Pb_2KNb_5O_{15}$ were examined as a function of the variables: liquid composition, cooling rates of grown crystals, size of crystals, and the design of the heat shields above the crucible. No major solution to this cracking problem was found, but a few fairly large crack free pieces have been obtained from some of the boules. Crystal growth of β-$LiAlSiO_4$ by flux methods was successful in that crystals of suitable size and quality for property measurements were obtained.

B. Measurement of Elastic, Thermoelastic, Piezoelectric and Dielectric Properties: The data analysis of previously started measurements of the elastic, thermoelastic and piezoelectric constants of $AlPO_4$, berlinite, was completed. Temperature compensated cuts on this material for bulk waves with orientations similar to those of AT and BT cuts in α-quartz are predicted and

show up to 250 percent larger electromechanical coupling than quartz. The five independent single crystal elastic constants of β-$LiAlSiO_4$, β-eucryptite, were measured as a function of temperature and pressure. The temperature and pressure coefficients of all elastic constants are negative. In spite of the negative thermal expansion coefficient parallel to the hexagonal axis no temperature compensated cuts exist, and on the basis of the measured piezoelectric stiffening contribution the electromechanical coupling is expected to be small. Therefore, β-eucryptite does not appear to be a suitable substitute for α-quartz.

(4) DoD Implications

The electromechanical coupling factor of α-berlinite has been found to be up to 250 percent larger than for α-quartz for bulk waves, and one may expect a significant improvement of the electromechanical coupling factor for surface acoustic waves as well. Thus by replacing quartz as a substrate material in surface acoustic wave (SAW) devices by berlinite insertion losses can be reduced and the operating frequency and/or bandwidth can be increased. In this manner the efficiency, reliability and capability of military communications and Radar systems utilizing SAW signal processing devices can be improved.

(5) Implications and Further Research

By demonstrating the superiority of α-berlinite over α-quartz for electromechanical device applications it has been shown that the search for new temperature compensated materials with properties superior to those of α-quartz through the approach used under the present contract is meaningful. One may therefore hope that a continued systematic search for new temperature compensated materials under the present contract may, even with the modest funding

level, eventually lead to the discovery of additional, perhaps even more suitable, materials.

(6) Specific Comments

No specific comments are offered at this time.

## Acknowledgments

The authors would like to thank their collaborators for their participation in this work: Dr. L. Drafall for most of the crystal growth work, Dr. Z. P. Chang for making the property measurements on berlinite, Mr. L. Bonczar for the crystal growth of and the property measurements on β-eucryptite, and Mr. W. B. Regnault for the crystal growth of lead potassium niobate.

## 1. Technical Problem

The objective of the research of this contract is to find temperature compensated materials for use in surface acoustic wave (SAW) signal processing devices, i.e. materials with large electromechanical coupling, low ultrasonic attenuation and a vanishingly small temperature coefficient of the delay time. The electromechanical coupling factor should be substantially larger than for α-quartz, which is presently used in temperature compensated SAW devices.

## 2. Methodological Approach

The research consists of: (A) both exploratory and systematic crystal growth studies on a variety of materials which are expected to be temperature compensated for bulk waves and which have been selected earlier under AFCRL Contract F19628-73-C-108 on the basis of certain heuristic criteria, and (B) measurements of the single crystal elastic and thermoelastic properties of the above grown crystals to determine whether they possess temperature compensated crystallographic directions for bulk waves, and measurements of piezoelectric and dielectric constants and their corresponding temperature coefficients to check the suitability of these materials for surface wave device applications.

### 2.1 Crystal Growth

The crystal growth research is being performed on materials grouping selected from the following list:

(1) $Ba_2Si_2TiO_8$
$Ba_2Ge_2TiO_8$
$Ba_2(Si,Ge)_2TiO_8$

(2) β-$LiAlSiO_4$

(3) $Pb_2KNb_5O_{15}$

(4) $Bi_2MoO_6$
$Bi_2WO_6$
$Bi_2(Mo,W)O_6$

(5) $Li_2SiO_3$
$Na_2SiO_3$
$(Li,Na)_2SiO_3$

(6) $Bi_2SiO_5$
$Bi_2GeO_5$
$Bi_2(Si,Ge)O_5$

(7) $Bi_2PbNb_2O_9$

(8) $NaAlSiO_4$
$KAlSiO_4$
$(Na,K)AlSiO_4$

Our approach is to use crystal pulling (Czochralski) and directional solidification (Bridgman) techniques for the growth of these materials whenever possible. These techniques usually yield the largest crystals with the least effort, but the compounds must melt congruently and must have reasonably low vapor pressures at the melting temperature. High temperature solution growth, i.e. flux techniques will be used on materials that do not meet the above requirements, and materials that readily solidify into glasses upon cooling their melts. A flux-pulling method will be tried first for these solution grown crystals.

We are attempting to first prepare the crystals that appear to be the easiest to grow so that samples will be available for property measurements. The order of the above material groupings is the approximate order in which the materials are being studied.

2.2 Measurement of Elastic, Thermoelastic, Piezoelectric and Dielectric Properties

Since the main purpose of the proposed work is to find new temperature compensated materials, the most important properties to be measured are the temperature coefficients of all single crystal elastic constants. We do this by means of ultrasonic velocity measurements as a function of temperature. For the evaluation of the temperature coefficients of the elastic constants from these data, the thermal expansion coefficients are also determined. They are also required for the calculation of the temperature coefficients of the bulk and surface mode delay times. If some of the effective elastic moduli which determine the ultrasonic velocities show positive temperature coefficients, a more complete assessment of the suitability of a given material for ultrasonic surface wave signal processing devices also requires the measurement of the piezoelectric and dielectric constants and their temperature coefficients. These measurements will be done either by the x-ray method or by the resonance

technique for the piezoelectric properties, and by means of the admittance bridge technique for the dielectric properties.

## 3. Technical Results

### 3.1 Crystal Growth

3.1.1 Barium Germanium Titanate: Our major crystal growth effort has centered on barium germanium titanate, $Ba_2Ge_2TiO_8$. Both Bridgman and Czochralski growth experiments have been carried out, but good crystals were obtained only in the latter pulling experiments.

Bridgman experiments were performed in attempts to duplicate the successful growth of $Ba_2Ge_2TiO_8$ reported by Kimura et al. (1), but all the boules obtained were cracked and milky in color. In attempting to remedy the poor quality of material obtained, better temperature control equipment was used, four different crucible lowering rates in the range of 0.5 to 3 mm/hr were tried, and temperature gradients near the freezing point goth breater and smaller and greater than 30°/inch were used. However, none of these changes resulted in crystal boules of even half decent quality. The reasons for these poor Bridgman results are not clear, and further attempts will not be pursued.

Czochralski crystal pulling experiments utilizing an rf-powered A.D. Little model M.P. crystal puller produced good quality single crystal boules except for a central core region which was vieled. In six of the seven growth experiments, the crystal was nucleated on a Pt or Pt/10% Rh wire 0.030 to 0.040 inches in diameter. The nature of the necking down procedure and the shape and size of an average crystal of $Ba_2Ge_2TiO_8$ grown in these studies can be seen from the xeroxed photograph shown in Fig. 1. A seed crystal was used in one experiment, but the quality of the resulting crystal was worse than when nucleation on the metal wire occurred. This was in spite of the fact

that the seed crystal was oriented in the same direction it was initially grown, and the seed was partially melted before the new crystal was grown.

In all of the crystals grown, a cloudy core was present which varied in size depending on the particular growth conditions. A scan with the electron microprobe across this region suggested a slight increase in

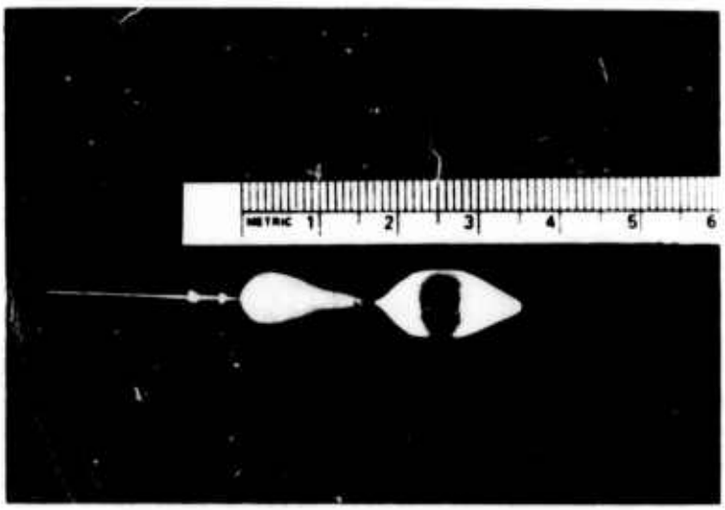


Figure 1. Typical $Ba_2Ge_2TiO_8$ Crystal Boule Pulled from Its Melt.

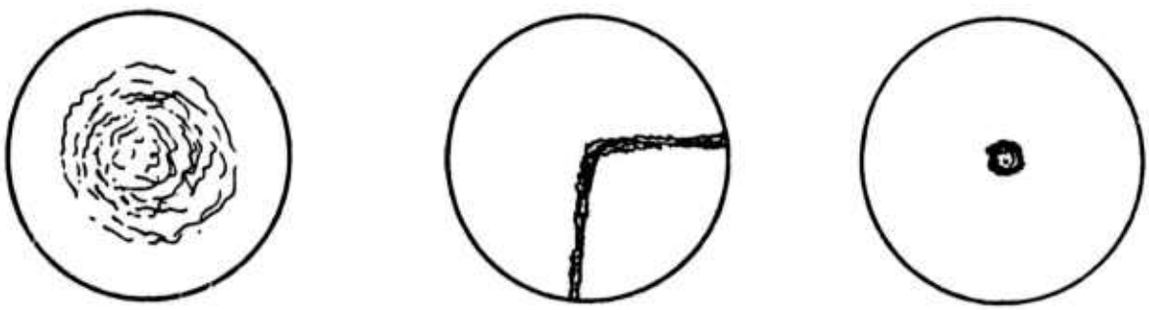

No. 2 - 20 rpm rotation
No crucible
insulation

No. 3 - 0 rpm rotation
crucible
insulated

No. 4 - 20 rpm rotation
crucible
insulated

Figure 2. Schematic Cross Sections of Crystals Grown Under Various Conditions of Crystal Rotation Rates and Crucible Insulation. The Size and Shape of the Cloudy Core Region is Indicated.

in germanium content, but these results are very tentative. The effects of crucible insulation and crystal rotation on the size and shape of the central core are illustrated in Fig. 2, which shows schematic cross sections of crystal boules.

During all the crystal pulling experiments on $Ba_2Ge_2TiO_8$, a small amount of material vaporized from the crucible and condensed in an amorphous state on the water-cooled chamber walls. A qualitative spectroscopic analysis of this material indicated the deposit was almost entirely germanium (probably $GeO_2$), with minor amounts of Pt (0.02 - 2%) and traces of Ti and Ba (<0.02%).

At present we are analyzing the information we have on the $Ba_2Ge_2TiO_8$ crystal growth and are preparing for experiments on $Ba_2Si_2TiO_8$. We have large enough quantities of good quality $Ba_2Ge_2TiO_8$ crystals for at least preliminary property measurements, and perhaps enough for all the measurements.

It was attempted to eliminate the central core imperfections in the grown crystals. We reasoned that if the central core was related to thermal losses or voltages set up across the platinum rod on which the crystal nucleates, then shortening and insulating this rod from the rest of the apparatus would have an effect on the core. We grew a crystal with an insulated rod, but noticed no effect on the core.

3.1.2 Barium Silicon Titanate (Fresnoite): Polycrystalline starting material of barium silicon titanate (fresnoite), $Ba_2Si_2TiO_8$, was synthesized by 1200°C heating of pressed pellets of the proper stoichiometric amounts of $BaCO_3$, $SiO_2$, and $TiO_2$. In growth experiments, the high melting point (reported to be 1360°C, but may be 50-100° higher) has caused problems in attaining sufficiently high temperatures in the center of an insulated platinum crucible without almost melting the crucible. Various heat shielding arrangements around the crucible were tried, as were various reflectors and shields above the crucible. Melting was attained and several crystal boules were obtained,

but they were of poor quality and were cracked extensively. Similar cracking problems were observed in the $Ba_2Ge_2TiO_8$ crystals when we attempted to use shields and reflectors above the crucible. Erosion of the platinum crucible through the formation of platinum oxides is relatively large. An iridium crucible is being considered so that we can go to higher temperatures without the top shielding, but crucible oxidation can be a problem in air. We ran growth experiments in argon with a platinum crucible to see if the titanium in the compound would be reduced to a trivalent state. Some reduction may be occurring, but this problem does not look severe.

3.1.3 Lead Potassium Niobate: Single crystal growth experiments on lead potassium niobate, $Pb_2KNb_5O_{15}$, that were started under a previous contract are continuing with the use of the rf-powered A. D. Little crystal puller. Although the procedures reported by Yamada (2) have been followed, the resulting crystal boules have cracked in many places, and the single crystal regions are twinned. Various shielding assemblies and cooling procedures have been tried without success. Several compositions either rich or poor in each of the respective components were prepared and studied in an attempt to understand more about the phase equilibria of the $PbO-K_2O-Nb_2O_5$ system, and thus understand the growth of the $Pb_2KNb_5O_{15}$ from molten compositions in this system.

In a recent paper by Nakano and Yamada (3) it is stated that good crystals were obtained from melts with compositions $Pb_{1.90-1.95}K_{1.2-1.1}Nb_5O_{15}$. Several runs were made using these compositions, but the results were the same as with other compositions richer in lead and poorer in potassium. Different cooling rates for the grown crystals were tried, but had little effect. Smaller diameter crystals were grown (6-8 mm), but cracking persisted. The shielding above the crucible was varied, and in a few runs removed, but the effects were small. Several fairly large crystal pieces have been obtained from the cracked boules, so several more runs will be made to see if enough large pieces can be

obtained to make property measurements on. Without a thorough phase and crystallographic study of this material, it appears that the cracking problem will not be conquered.

3.1.4 β-Eucryptite: The crystal growth of β-eucryptite, β-$LiAlSiO_4$, also begun on a previous contract was successfully completed, and crystal large enough for property measurements were obtained. Winkler's method (4) of using a lithium cryolite flux was followed, and yielded single crystals with linear dimensions up to 10 mm and volumes up to about 200 $mm^3$. The crystals obtained are transparent and appear to be of good quality and relatively free of inclusions.

3.2 Elastic, Thermoelastic and Piezoelectric Properties

3.2.1 α-Berlinite: Our work on α-berlinite, α-$AlPO_4$, begun under a previous contract, has been completed, and the results have been submitted for publication (5).

The six single crystal elastic constants of α-berlinite (crystal class $D_3(32)$) have been measured by means of the ultrasonic pulse superposition method between 80 and 293°K, and the thermal expansion behavior has been determined from 293 to 950°K by the x-ray powder diffraction method through the α-β transition at about 857°K. The specimens used were cut from a crystal which had been grown hydrothermally at the Signal Corps Engineering Laboratories, Fort Monmouth, New Jersey.

The thermal expansion data indicate an abrupt change in the lattice parameters at about 584°C, resulting from the α-β transformation, and are qualitatively and quantitatively very similar to those for quartz (6). In Table I the room temperature values of the two lattice parameters, of the linear thermal expansion coefficients and of the temperature coefficients of the linear thermal expansion coefficients are listed. For the lattice parameter

a the data from 23° to 397°C, and for c the data from 23° to 556°C were included in the least squares fit. The lattice parameters agree very well with the values reported before for berlinite (7) (a=4.942Å and c=10.97Å). The linear thermal expansion coefficients perpendicular and parallel to the trigonal axis are 17 percent and 34 percent larger than for α-quartz (6,8) respectively.

Table I Lattice parameters (at 296°K), linear thermal expansion coefficients, and temperature coefficients of the linear thermal expansion coefficients (at 298°K) for berlinite

| L | a | c |
|---|---|---|
| L(Å) | 4.943 | 10.974 |
| $\alpha = \frac{1}{L}(\frac{\partial L}{\partial T})$ $(10^{-5}°K^{-1})$ | 1.59 ± 0.06 | 0.97 ± 0.11 |
| $\frac{d\alpha}{dT}$ $(10^{-8}°K^{-2})$ | 1.5 ± 0.6 | 1.5 ± 0.8 |

As for α-quartz, the elastic constants $c_{11}^E$, $c_{33}^E$, $c_{44}^E$, $c_{12}^E$ and $c_{13}^E$ decrease with increasing temperature, but the shear modulus $c_{66}^E$ and the modulus $|c_{14}^E|$ increase with increasing temperature. The transit time for the X-cut shear mode, polarized parallel to the Y-direction shows a minimum at about -8°C. On the other hand Mason (9) reported a maximum for the resonance frequency of the Y-cut thickness shear mode, polarized parallel to the X-direction, at -40°C. This result is in contradiction to our own data, which show that the directly measured transit time for this mode decreases monotomically with increasing temperature. It is suggested that the discrepancy arises from mode coupling effects in the resonance type experiments of Mason (9).

In Table II the room temperature values of the elastic constants and their temperature derivatives are compared with the corresponding data for α-quartz. Also included are the elastic constants of $AlPO_4$ obtained by Mason (9,10). It is apparent that, with the exception of $c_{14}$, the present data differ significantly from those of Mason (9,10). With the exception of $c_{44}$, the present data are considerably smaller than Mason's results. Although Mason's data were obtained by means of the resonance technique the large difference cannot be attributed to the different experimental methods used. One possible explanation is perhaps that the sample measured by Mason was not pure stoichiometric $AlPO_4$. On the other hand, the present results are systematically smaller than the data for quartz, with the differences (referred to quartz) smaller than about 25 percent.

Most of the temperature derivatives of the elastic constants of $AlPO_4$ are less than half the values for $SiO_2$, except for $c_{44}$, which is only 33 percent smaller, and for $c_{11}$ and $c_{33}$ which are up to 25 percent larger.

The eigenvalues of the ultrasonically measured Christoffel tensor contain, in addition to the elastic constants $c^E_{\mu\nu}$, piezoelectric stiffening terms, which depend on the piezoelectric and dielectric constants. Since in our investigations twelve independent modes were measured as a function of temperature, the stiffening terms could be separated from the six independent elastic constants. In order to obtain the piezoelectric constants and their dependence on temperature from the piezoelectric stiffening terms the dielectric constants and their temperature dependence must be known, respectively.

Approximate room temperature values of the piezoelectric stress constants $e_{i\mu}$ were obtained by using a value of $\varepsilon^S_{11} = 5.88$, calculated from the value of the dielectric constant for constant stress, $\varepsilon^T_{11} = 6.05$ given for $AlPO_4$ by Mason (9), and by assuming $\varepsilon^S_{11} = \varepsilon^S_{33}$. The results are listed in Table III

Table II Comparison of present results for elastic constants (in $10^2$ dynes/cm$^2$) and their temperature derivatives (in $10^8$ dynes/cm$^2$ °K) for $\alpha$-$AlPO_4$ with the corresponding data for $\alpha$-$SiO_2$ and with other elastic constant data for $\alpha$-$AlPO_4$ at 298°K.

| | | 11 | 33 | 44 | 66 | 12 | 13 | 14 |
|---|---|---|---|---|---|---|---|---|
| $c^E_{\mu\nu}$ | $AlPO_4$ (present) | 0.640 ±.007 | 0.858 ±.003 | 0.432 ±.003 | 0.284 ±.006 | 0.072 ±.013 | 0.096 ±.006 | -0.124 ±.003 |
| | $AlPO_4$ [a] | 1.050 | 1.335 | 0.231 | 0.379 | 0.293 | 0.693 | -0.127 |
| | $SiO_2$ [b] | 0.869 | 1.058 | 0.582 | 0.399 | 0.0714 | 0.120 | -0.181 |
| $(\partial c^E_{\mu\nu}/\partial T)_p$ | $AlPO_4$ (present) | -0.485 ±.016 | -1.87 ±.03 | -0.677 ±.018 | +0.292 ±.013 | -1.07 ±.03 | -0.38 ±.01 | -0.089 ±.010 |
| | $SiO_2$ [c] | -0.385 | -1.693 | -1.021 | -0.748 | -1.92 | 0.66 | -0.21 |

[a] Calculated by Bechmann, reference (10), from elastic compliance data of Mason, reference (7).

[b] McSkimin, reference (9).

[c] Zelenka and Lee, reference (11).

Table III Piezoelectric stress constants $e_{i\mu}$ (in $C/m^2$) and their temperature coefficients $(\partial e_{i\mu}/\partial T)_p$ (in $10^{-4}$ $C/m^2$ °K) for $\alpha$-$AlPO_4$ and $\alpha$-$SiO_2$. The sign of $e_{11}$ for $AlPO_4$ was chosen so as to agree with that for dextrorotary $\alpha$-$SiO_2$.

| $i\mu$ | | 11 | 14 |
|---|---|---|---|
| $e_{i\mu}$ | $\alpha$-$AlPO_4$ (present[a]) | -0.30 | 0.13 |
| | $\alpha$-$AlPO_4$[b] | -0.27 | 0.12 |
| | $\alpha$-$SiO_2$[c] | -0.17 | 0.040 |
| $(\partial e_{i\mu}/\partial T)_p$ | $\alpha$-$AlPO_4$ (present[a,d]) | 0.80 | -0.73 |
| | $\alpha$-$SiO_2$[e] | 0.27 | -0.58 |

[a]Calculated from $\varepsilon_{11}^S = 5.88$ (calculated from $\varepsilon_{11}^T = 6.05$; Mason, reference (12)) on the basis of the assumption $\varepsilon_{11}^S = \varepsilon_{33}^S$.

[b]Calculated from the piezoelectric strain constants and from the elastic constants of Mason, reference (12).

[c]Bechmann, reference (13).

[d]Calculated by using the relative temperature coefficients $(1/\varepsilon_{ii}^S)(\partial\varepsilon_{ii}^S/\partial T)_p (i=1,3)$ of the dielectric constants for $\alpha$-quartz from reference (10).

[e]Bechmann, reference (14).

and are seen to agree within about ten percent with the values calculated from the piezoelectric strain constants given by Mason (9). The constant $e_{11}$ is almost two times, and $e_{14}$ almost three times larger than the corresponding values for $\alpha$-$SiO_2$. Considerably smaller values of the piezoelectric stress constants were given by other authors (15,16) but this may be due to the presence of micro-twinning.

Since the temperature coefficients of the dielectric constants of berlinite are not known, and since these quantities represent only a small correction in the calculation of the temperature coefficients of the piezoelectric constants from the piezoelectric stiffening terms, the values for $\alpha$-quartz were used. They are (10): $(1/\varepsilon_{11}^S)(\partial\varepsilon_{11}^S/\partial T)_p = 0.28$ and $(1/\varepsilon_{33}^S)(\partial\varepsilon_{33}^S/\partial T)_p = 0.39$ (in $10^{-4}(°K)^{-1}$). Temperature coefficients of the piezoelectric constants obtained in this manner are also listed in Table III and are for $e_{11}$ three times, and for $e_{14}$ 26 percent larger than for $\alpha$-$SiO_2$.

The round trip delay time of an ultrasonic wave travelling through a piezoelectric crystal plate of thickness t and in the direction $\bar{N}$ is given by

$$\tau = 2t/V \tag{1}$$

where

$$V = \sqrt{c/\rho} \tag{2}$$

is the ultrasonic velocity as determined from the eigenvalues $\bar{c} = \bar{c}(\bar{N})$ of the Christoffel tensor, with the piezoelectric stiffening terms included.

By differentiation of equ. (1) the temperature coefficient of the transit time can be expressed in terms of the volume thermal expansion coefficient $\alpha_v$, the linear thermal expansion coefficient $\alpha = \alpha(\vec{N})$ and the effective elastic constant $\bar{c}$ through the expression

$$\frac{1}{\tau}\left(\frac{\partial\tau}{\partial T}\right)_p = \alpha - \frac{1}{2}\alpha_v - \frac{1}{2\bar{c}}\left(\frac{\partial\bar{c}}{\partial T}\right)_p \tag{3}$$

For small electromechanical coupling factor the resonance frequency f of the same crystal plate is given by the reciptrocal of the transit time, so that $(1/f)(\partial f/\partial T) = -(1/\tau)(\partial \tau/\partial T)$. For large electromechanical coupling factor the resonance frequency of an uncoupled mode is given by (17)

$$f = (V/\pi t)X \tag{4}$$

where X is the solution of

$$\tan X = X/k^2 \tag{5}$$

and where k is the electromechanical coupling factor.

In order to investigate the existence of temperature compensated directions in $AlPO_4$ the round trip delay time $\tau$, the resonance frequency f and the temperature coefficient of both quantities have been calculated as a function of orientation for the rotated Y-cut thickness-shear mode, assuming a plate thickness t = 1 mm. In a crystal plate with infinite lateral dimensions this mode is for all angles of rotation around the X-axis independent of the other two solutions of the Christoffel tensor. The effective elastic constant is for this mode given by (17)

$$\bar{c}_{66} = c'_{66} + \frac{(e'_{26})^2}{\varepsilon'_{22}} \tag{6}$$

The electromechanical coupling factor is given by (17)

$$k^2 = \frac{(e'_{26})^2}{\bar{c}_{66}\,\varepsilon'_{22}} \tag{7}$$

The elastic, piezoelectric and dielectric constants for the rotated crystal are given by

$$c'_{66} = c_{66}\,x^2 + c_{44}\,y^2 + 2c_{14}xy \qquad (8a)$$

$$e'_{26} = -\,(e_{11}\,x + e_{14}\,y)x \qquad (8b)$$

$$\varepsilon'_{22} = \varepsilon^S_{11}\,x^2 + \varepsilon^S_{33}\,y^2 \qquad (8c)$$

where $x = \cos\phi$ and $y = \sin\phi$, and $\phi$ denotes the rotation angle around the X-axis according to the IRE standards (18).

In Figs. 3 and 4 the results for the delay time and for the resonance frequency, respectively, are shown as a function of rotation angle. The plots in Fig. 4 are qualitatively very similar to the corresponding plots for α-quartz (19). The resonance frequency passes through a maximum at -60°, and a minimum at 29°. The rotation angles for the corresponding BC and AC cuts in α-quartz are -58° and 31°, respectively. At -44° and at 30° the temperature coefficient of the resonance frequency passes through zero. In α-quartz the orientations for the corresponding BT and AT cuts are -51° and 35°, respectively. Comparison with Fig. 3 shows that the angles for the minimum and maximum of the delay time, corresponding to the orientations denoted by BC' and AC', differ by only one or two degrees from those for the BC and AC cuts referring to the resonance frequency. The same is true for the orientation of the AT' and AT cuts. However, the angles for the BT' and BT cuts differ by about 7°.

In Fig. 5 the calculated orientation dependence of the electromechanical coupling factor is shown. The values of the coupling factor for α-quartz corresponding to the four cuts indicated in the graph are 0.040 (BC), 0.054 (BT), 0.098 (AC) and 0.089 (AT). From Fig. 5 it is apparent that the corresponding coupling factors for α-berlinite are up to 250 percent larger than for α-quartz. As for α-quartz, other temperature compensated directions exist which are in general of less practical use because of mode coupling and/or smaller electromechanical coupling factor. For example, for the

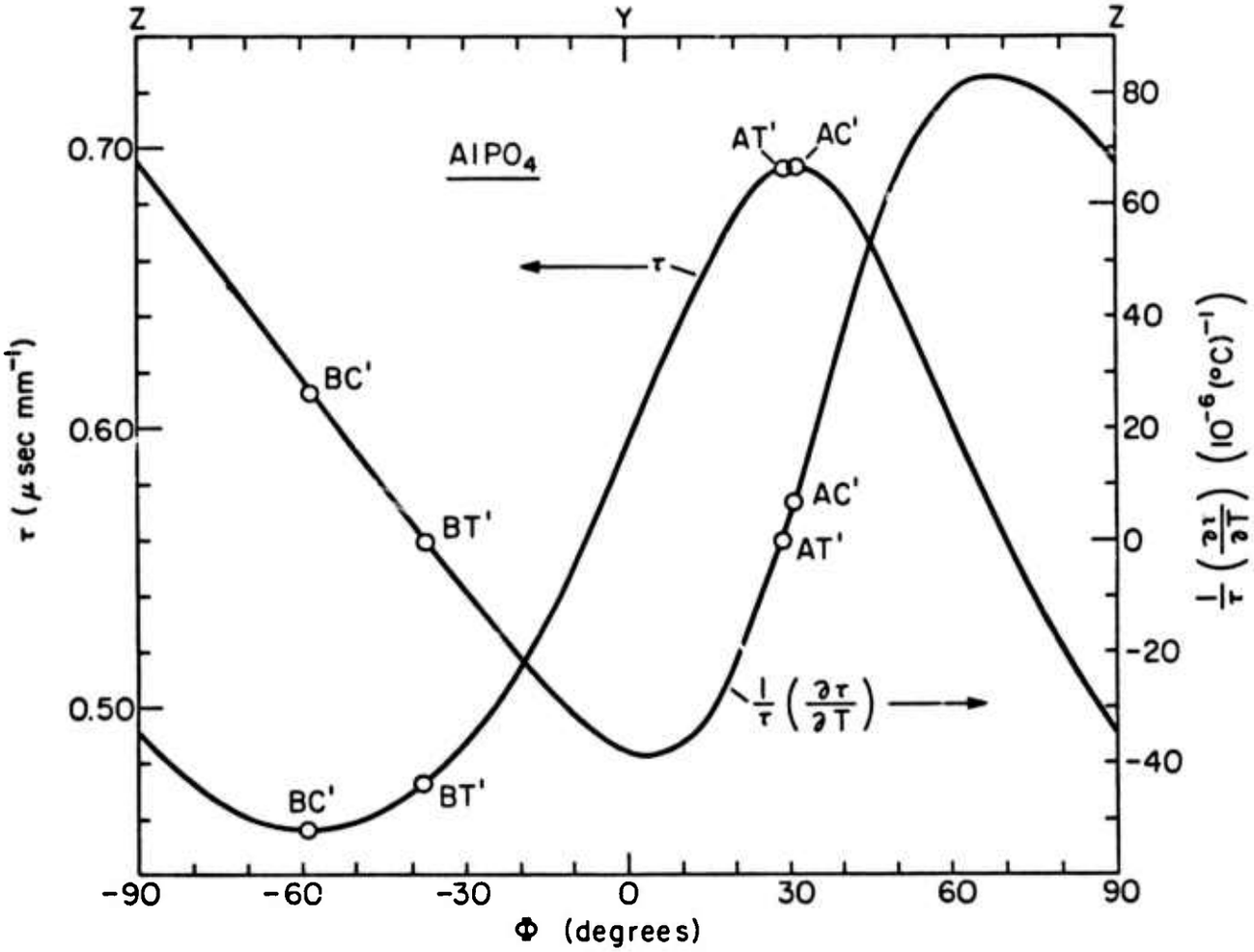


Fig. 3

Calculated round trip delay time τ for plate thickness of 1 mm, and temperature coefficient $(1/\tau)\,(\partial\tau/\partial T)$ for rotated Y-cut crystal versus angle of rotation Φ.

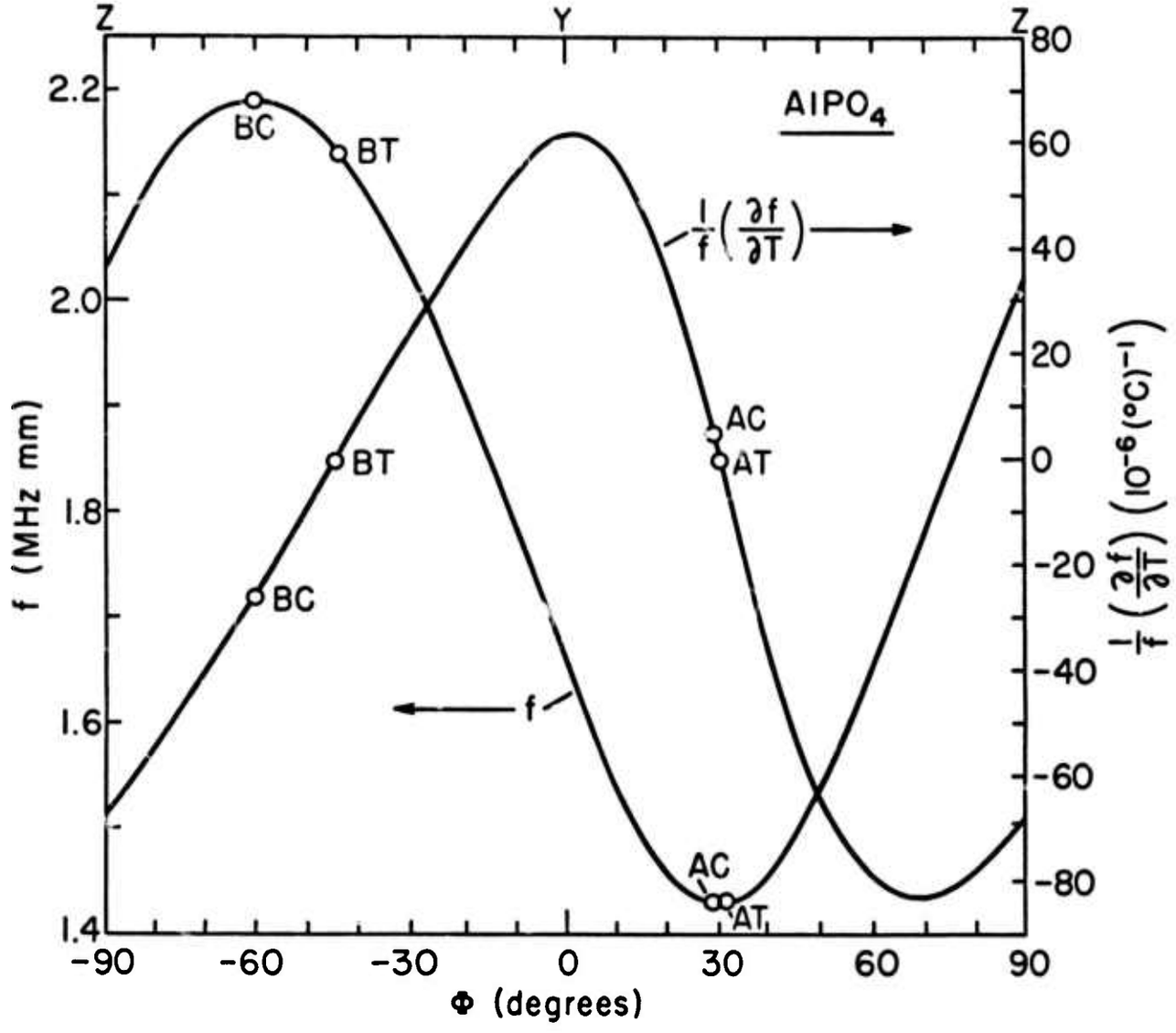


Fig. 4

Calculated frequency constant f and its temperature coefficient (1/f) (∂f/∂T) for rotated Y-cut crystal versus angle of rotation Φ.

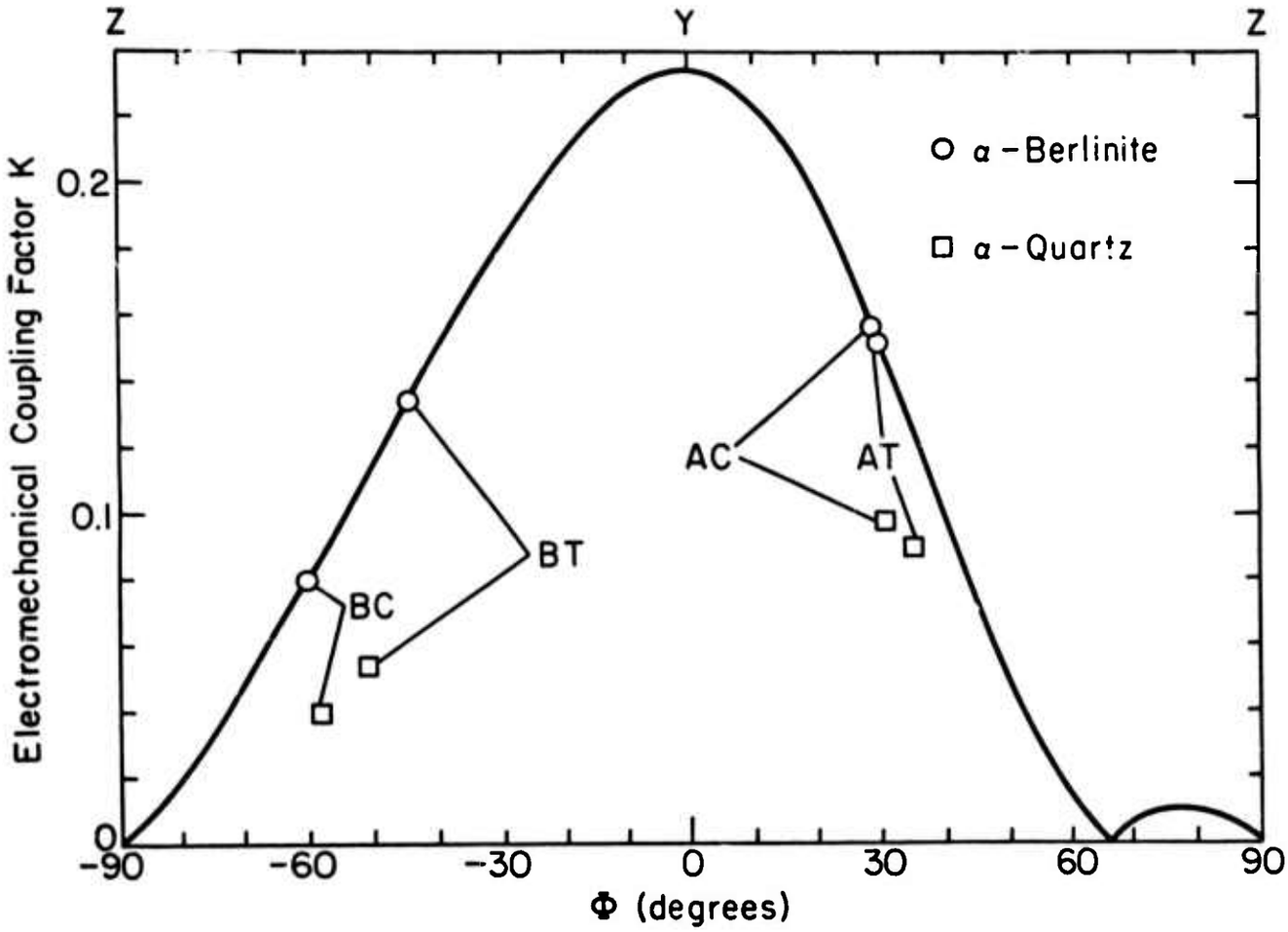


Fig. 5

Calculated electromechanical coupling factor k for rotated Y-cut crystal versus angle of rotation $\Phi$.

X-cut rotated by ±2.5° around the Y-axis the temperature coefficient of the delay time is zero, but the electromechanical coupling is very small.

The results of Figs. 4 and 5 suggest that α-berlinite may be a more suitable piezoelectric material for use in bulk wave ultrasonic devices that α-quartz, as the larger electromechanical coupling would lead to lower insertion losses, higher frequency limit, and larger bandwidth. For the substantiation of this conclusion a more accurate determination of the piezoelectric constants and the direct measurement of their temperature dependence and of the dielectric constants and their temperature dependence are required.

3.2.2 β-Eucryptite: The five single crystal elastic constants of β-eucryptite, β-$LiAlSiO_4$ (crystal class $D_6(622)$), their temperature coefficients and their pressure coefficients have been measured by means of the ultrasonic pulse superposition method. The results are listed in Table IV and show that all pressure and temperature coefficients are negative.

By making measurements for 8 independent modes it was also possible to obtain the piezoelectric stiffening contribution to the effective elastic constants, as well as the temperature and pressure derivatives of this quantity. Since very recently the dielectric constants of β-eucryptite have been measured as a function of temperature and frequency (20), it was possible to calculate the piezoelectric constant $e_{14}$ and its temperature coefficient from the stiffening term. Using the approximate values corresponding to 20 MHz (20)

$$\varepsilon_{11} = 85 \; ; \quad \varepsilon_{33} = 500$$

$$(\partial\varepsilon_{11}/\partial T) = 0.1(°K)^{-1} \; ; \quad (\partial\varepsilon_{33}/\partial T) = 10(°K)^{-1} \, ,$$

one obtains (at 20°C):

$$e_{14} = 1.76 \text{ Coul/m}^2 \; ; \; (\partial e_{14}/\partial T) = 0.019 \text{ Coul/m}^2 °K$$

Table IV

Adiabatic Second Order Elastic Constants ($10^{12}$ $\frac{\text{dynes}}{\text{cm}^2}$), Their Isothermal First Pressure Derivatives (dimensionless) and Their Isobaric Temperature Derivatives ($10^{7}$ $\frac{\text{dynes}}{\text{cm}^2}$) of Beta-Eucryptite at 25°C.

| $\mu\nu$ | 11 | 44 | 66 | 33 | 12 | 13 |
|---|---|---|---|---|---|---|
| $c^E_{\mu\nu}$ | 1.258 ±.002[a] | .568 ±.001[a] | .480 ±.002[a] | .962 ±.002[a] | .298 ±.004[a] | .587 ±.001[b] |
| $\left(\frac{\partial c^E_{\mu\nu}}{\partial p}\right)_T$ | -3.74 ±.10[a] | -1.33 ±.03[a] | -.63 ±.03[a] | -.49 ±.06[a] | -2.48 ±.12[a] | -.95 ±.11[b] |
| $\left(\frac{\partial c^E_{\mu\nu}}{\partial T}\right)_p$ | -14.4 | -11.3 | -3.3 | -14.2 | -7.9 | -13.6 |

[a]Standard Error from Simultaneous Least Squares Fit of Seven Equations for Five Unknowns.

[b]Calculated from Gaussion Error Propagation Law.

According to equ. (3) the temperature coefficient of the delay time may be zero even for materials with negative temperature coefficients of the elastic constants, provided the quantity $\alpha-\alpha_v/2$ is negative and large enough, so as to cancel the last term in equ. (3). For β-eucryptite the two linear expansion coefficients are (21,22):

$$\alpha_{||} = -\ 18.4 \times 10^{-6}\ (°C)^{-1}$$

$$\alpha_{\perp} = +\ 8.6 \times 10^{-6}\ (°C)^{-1}$$

Because of the large negative value of $\alpha_{||}$, the thermal expansion coefficient in the direction of the hexagonal axis, it would appear that such a cancellation of all terms in equ. (3) is possible. Therefore the transit time $\tau$, the resonance frequency f, and the temperature coefficients of these two quantities were calculated as a function of direction $\bar{N}$ = (cos $\phi$ sin $\theta$, sin $\phi$ sin $\theta$, cos $\theta$) for the following cases:

(1) $\theta = 90°$ , $\phi$ variable

(2) $\phi = 0°$ , $\theta$ variable

(3) $\phi = 30°$ , $\theta$ variable

(4) $\phi = 60°$ , $\theta$ variable

For none of these directions did the temperature coefficients of the transit time or of the resonance frequency become zero. However, the angular dependence of the temperature coefficients exhibit rather sharp minima, and the values of the temperature coefficients at these minima are very small $((1/\tau)(\partial\tau/\partial T) = 4 \times 10^{-6}(°K)^{-1}$ for $\theta = 40°$ and $\theta = 140°$, with $\phi = 0°$, 30°, 60°). Thus it appears that for bulk waves β-eucryptite is almost a temperature compensated material. The existence of temperature compensated cuts for surface waves, however, cannot be ruled out altogether and requires appropriate computer calculations.

The electromechanical coupling factor for the thickness-shear mode of the rotated Y-cut as defined in equ. (7) was calculated as a function of direction and found to show a maximum of k = 0.027 at an angle of 32° 40' with the Y-axis. This value is considerably smaller than the coupling factor for the temperature compensated cuts of α-quartz (0.054 for BT and 0.089 for AT). Although the value for β-eucryptite is subject to a large experimental error, because the piezoelectric stiffening term is experimentally determined as the difference between two large numbers, it is unlikely that an independent more direct determination of the piezoelectric constant $e_{14}$ will drastically alter this result.

Another undesirable property of β-eucryptite are rather large dielectric losses parallel to the hexagonal axis (20). At 30°C the loss tangent decreases from a value of 1.2 for 30 Hz to a value of 0.1 for $10^5$ Hz (20).

Based on the available evidence one may conclude with a high degree of probability that β-eucryptite is not a suitable temperature compensated piezoelectric material for use in bulk or surface acoustic wave devices. However, this tentative conclusion needs to be substantiated through independent measurement of the piezoelectric constant and its temperature coefficient.

Although β-eucryptite, β-$LiAlSiO_4$, itself appears to be of no immediate practical interest it may be a useful starting material for improving its properties through compositional variations. For example, partial substitution of Ge for Si (up to 20 percent) does not affect the anomalous thermal expansion behaviour (23), and it is conceivable that with only slightly different temperature coefficients of the elastic constants the temperature coefficient of the bulk mode delay time will become zero.

It is apparent from equ. (7) that the large values of the two dielectric constants, especially of $\varepsilon_{33}$, are the cause for the small electromechanical coupling factor. If it were possible to reduce the dielectric constant without much reduction of the (relatively large) piezoelectric constant $e_{14}$ the electromechanical coupling factor could be substantially increased. Since the large dielectric constant and the large dielectric losses in β-eucryptite have been attributed to the large mobility of Li ions along the open channels in the direction of the hexagonal axis (20) one may expect that both quantities may be reduced by partial substitution of Li by heavier alkali metal ions, such as Na. Neither the solid-solubility range nor the effect of such substitution on the elastic and thermoelastic properties are known at this time.

The anomalous thermal expansion behaviour poses, of course, an interesting challenge to understand this behaviour in terms of composition, crystal structure and chemical bond. Such an understanding could initiate a search for other crystal structures and materials with similar, but otherwise more favourable properties.

As a first step in this direction one may calculate the Grueneisen parameter on the basis of the anisotropic elastic continuum model (24). The Grueneisen parameter obtained in this manner is given by

$$\gamma_{el} = \langle \gamma_i \rangle \tag{9}$$

with the mode gamma defined as

$$\gamma_i = - (\partial \ln \omega_i / \partial \ln V) \tag{10}$$

Here $\omega_i$ denotes the frequency of the ith mode, and V the volume of the crystal. In the anisotropic elastic continuum model (24) the frequencies are expressed in terms of the elastic constants, the mode gammas $\gamma_i$ are expressed in terms of the pressure derivatives of the elastic constants, and the mode average in

equ. (9) is extended only over the three acoustic branches, thereby neglecting dispersion and all optical modes. In Table V the results calculated in this manner from the elastic data of Table IV are compared with the thermal Grueneisen parameter,

$$\gamma = \frac{\beta B^S}{\rho C_p} \tag{11}$$

($\beta$ = volume thermal expansion coefficient, $B^S$ = adiabatic bulk modulus, $\rho$ = density, $C_p$ = specific heat for constant pressure). For the specific heat a value of $C_p$ = 1.312 joule/g°K was used, which was calculated from the elastic Debye temperature of $\theta$ = 314.1 °K.

Table V Comparison of elastic and thermal Grueneisen parameters of β-eucryptite

| | Elastic | Thermal |
|---|---|---|
| $\gamma_o$ | -1.59 | unknown |
| $\gamma_\infty$ | -1.07 | -0.050 |

It is apparent that in the high temperature limit the elastic Grueneisen parameter reproduces the negative sign of the thermal Grueneisen parameter, but its magnitude is 20 times larger. This may be attributed to the omission of dispersion and of the optical modes in the anistropic elastic continuum model (24). One may conclude therefore, that on the average the omitted modes have positive mode gammas. On the other hand, the low temperature limit of the thermal Grueneisen parameter must agree with the long wavelength elastic limit calculated in the anisotropic elastic continuum approximation, so that

one may predict a strong temperature dependence and considerably more negative values of the thermal Grueneisen parameter at low temperature.

In order to account for the Grueneisen parameters $\gamma_{||}$ and $\gamma_{\perp}$ corresponding to the individual linear thermal expansion coefficients $\alpha_{||}$ and $\alpha_{\perp}$ on the basis of the anisotropic continuum model the third order elastic constants must be known (24).

The occurrence of all negative signs of the pressure coefficients is unique among crystalline solids, as pressure coefficients of elastic constants normally are positive, and no other crystalline material with all negative pressure coefficients is known. The negative pressure coefficients have implications for the high-pressure phase diagrams and suggest the existence of several distinct (stable or metastable) high-pressure phases. In fact, a transformation of 8 kbar to an as yet unidentified phase has been very recently observed by Morosin and Peercy (25), and Neuhaus and Meyer (26) report that between 30 to 55 kbar and at 1000°C α-eucryptite decomposes into α-spodumene and lithium aluminate.

## 3.3 References

(1) M. Kimura, K. Doi, S. Nanamatsu and T. Kawamura. A New Piezoelectric Crystal: $Ba_2Ge_2TiO_8$, Appl. Phys. Lett. 23, 531 (1973).

(2) T. Yamada. Single-Crystal Growth and Piezoelectric Properties of Lead Potassium Niobate, Appl. Phys. Lett. 23, 213 (1973).

(3) J. Nakano and T. Yamada. Ferroelectric and Optical Properties of Lead Potassium Niobate, J. Appl. Phys. 46, 2361 (1975).

(4) H. G. F. Winkler. Synthese und Kristallstruktur des Eukryptits, $LiAlSiO_4$, Acta Cryst. 1, 27 (1948).

(5) Z. P. Chang and G. R. Barsch. Elastic Constants and Thermal Expansion of Berlinite, IEEE Transactions on Sonics and Ultrasonics, accepted for publication (1975).

(6) A. H. Jay. The Thermal Expansion of Quartz by X-Ray Measurements, Proc. Roy. Soc. A142, 237-247 (1933).

(7) R. W. G. Wyckoff. Crystal Structures, Vol. 3, p. 31, Interscience Publishers (1965).

(8) R. K. Kirby, T. A. Hahn and B. D. Rothrock. Thermal Expansion, in D. E. Gray, Ed., American Institute of Physics Handbook, p. 4-119 to 4-142, McGraw-Hill (1972).

(9) W. P. Mason. Piezoelectric Crystals and Their Applications to Ultrasonics, p. 208, Van Nostrand (1950).

(10) R. Bechmann. The Elastic, Piezoelectric and Dielectric Constants of Piezoelectric Crystals, in Landolt-Börnstein, Group III, Vol. 1, Eds. K. H. Hellwege and A. M. Hellwege, p. 40-123, Springer (1966).

(11) J. Zelenka and P. C. Lee. On the Temperature Coefficients of the Elastic Stiffnesses and Compliances of Alpha-Quartz, IRE Trans. Sonics Ultrasonics SU18, 79-80 (1971).

(12) W. P. Mason. Piezoelectric Crystals and Their Application to Ultrasonics, p. 208, Van Nostrand (1950).

(13) R. Bechmann. Elastic and Piezoelectric Constants of Alpha-Quartz, Phys. Rev. 110, 1060-1061 (1958).

(14) R. Bechmann. Temperaturabhängigkeit von Quarzresonatoren, Arch. Elektr. Übertragung 5, 89-90 (1951). Quoted in reference 6.

(15) J. M. Stanley. Hydrothermal Synthesis of Large Aluminum Phosphate Crystals, Ind. Eng. Chem. 32, 1684-1689 (1954).

(16) H. J. Jaffe. The Brush Development Co., Cleveland, Ohio. U.S. Signal Corps Contract Nr. W-28-003-SC-1583, Final Report 1 April 1948. Quoted in reference (10).

(17) H. F. Tiersten. Thickness Vibrations of Piezoelectric Plates, J. Acoust. Soc. Am. 35, 53-58 (1963).

(18) Standards on Piezoelectric Crystals, Proc. IRE 14, S1, 1378-1395 (1949).

(19) W. P. Mason. Piezoelectric Crystals and Their Applications to Ultrasonics, p. 99, Van Nostrand (1950).

(20) H. Böhm. Dielectric Properties of β-Eucryptite, phys. stat. Sol. (a) 30, 531 (1975).

(21) F. A. Hummel. Thermal Expansion Properties of Some Synthetic Lithia Minerals, J. Am. Ceram. Soc. 34, 235 (1951).

(22) H. Schulz. Thermal Expansion of Beta Eucryptite, J. Am. Ceram. Soc. 57, 313 (1974).

(23) T. Y. Tien and F. A. Hummel. Studies in Lithium Oxide Systems: XIII, $Li_2O \cdot Al_2O_3 \cdot 2SiO_2$ - $Li_2O \cdot Al_2O_3 \cdot 2GeO_2$, J. Am. Ceram. Soc. 47, 582 (1964).

(24) K. Brugger. Grueneisen Gamma from Elastic Data, Phys. Rev. 157, 524 (1967).

(25) B. Morosin and P. S. Peercy. Pressure-Induced Phase Transition in β-Eucryptite ($LiAlSiO_4$), Physics Letters 53A, 147 (1975).

(26) A. Neuhaus and H. J. Meyer. Hochdruckverhalten des Eukryptits (α-$LiAlSiO_4$) und anderer oxydischer Phasen, Naturwiss. 52, 639 (1965).